

Published in final edited form as:

Bone. 2013 November ; 57(1): . doi:10.1016/j.bone.2013.08.018.

Anti-resorptive Agents Reduce the Size of Resorption Cavities: A Three-Dimensional Dynamic Bone Histomorphometry Study

J.B. Matheny^{1,2}, C.R. Slyfield¹, E.V. Tkachenko¹, I. Lin¹, K.M. Ehlert¹, R.E. Tomlinson⁴, D.L. Wilson⁴, and C.J. Hernandez^{1,2,3}

¹Sibley School of Mechanical and Aerospace Engineering, Cornell University, Ithaca, NY, USA

²Department of Biomedical Engineering, Cornell University, Ithaca, NY, USA

³Hospital for Special Surgery, New York, NY, USA

⁴Department of Biomedical Engineering, Case Western Reserve University, Cleveland, OH, USA

Abstract

Alterations in resorption cavities and bone remodeling events during anti-resorptive treatment are believed to contribute to reductions in fracture risk. Here, we examine changes in the size of individual remodeling events associated with treatment with a selective estrogen receptor modulator (raloxifene) or a bisphosphonate (risedronate). Adult female rats (6 months of age) were submitted to ovariectomy (n = 17) or sham surgery (SHAM, n = 5). One month after surgery, the ovariectomized animals were separated into three groups: untreated (OVX, n = 5), raloxifene treated (OVX+Ral, n = 6) and risedronate treated (OVX+Ris, n = 6). At 10 months of age, the lumbar vertebrae were submitted to three-dimensional dynamic bone histomorphometry to examine the size (depth, breadth, volume) of individual resorption cavities and formation events. Maximum resorption cavity depth did not differ between the SHAM ($23.66 \pm 1.87 \mu\text{m}$, mean \pm SD) and OVX ($22.88 \pm 3.69 \mu\text{m}$) groups but was smaller in the OVX+Ral ($14.96 \pm 2.30 \mu\text{m}$) and OVX+Ris ($14.94 \pm 2.70 \mu\text{m}$) groups ($p < 0.01$). Anti-resorptive treatment was associated with reductions in the surface area of resorption cavities and the volume occupied by each resorption cavity ($p < 0.01$ each). The surface area and volume of individual formation events (double-labeled events) in the OVX+Ris group were reduced as compared to other groups ($p < 0.02$). Raloxifene treated animals showed similar amounts of bone remodeling (ES/BS and dLS/BS) compared to sham-operated controls but smaller cavity size (depth, breadth and volume). The current study shows that anti-resorptive agents influence the size of resorption cavities and individual remodeling events and that the effect of anti-resorptives on individual remodeling events may not always be directly related to the degree of suppression of bone remodeling.

© 2013 Elsevier Inc. All rights reserved.

Corresponding Address: Christopher J. Hernandez, Ph.D., 219 Upson Hall, Cornell University, Ithaca, NY 14853 Phone: (607) 255-5129, Fax: (607) 255-1222, cjh275@cornell.edu.

Publisher's Disclaimer: This is a PDF file of an unedited manuscript that has been accepted for publication. As a service to our customers we are providing this early version of the manuscript. The manuscript will undergo copyediting, typesetting, and review of the resulting proof before it is published in its final citable form. Please note that during the production process errors may be discovered which could affect the content, and all legal disclaimers that apply to the journal pertain.

Conflict of Interest Statement: Dr. Wilson has an interest in BioInVision, Inc. which may commercialize the image acquisition/analysis approach. All other authors have no disclosures relevant to the current manuscript.

Ethical Review Board Statement: The animal work in the study described was performed under the approval of the Case Western Reserve University IACUC.

Keywords

Bone Remodeling; Bone Histomorphometry; Ovariectomy; Osteoporosis; Bisphosphonates; SERMS

1.0 INTRODUCTION

Anti-resorptive agents are the most commonly used type of pharmacological treatment for osteoporosis. Reductions in fracture risk from anti-resorptive treatments, however, are greater than would be expected from the associated increases in bone mineral density (BMD) caused by treatment [1, 2]. The causes for the disproportionate reduction in fracture risk associated with anti-resorptive treatment are not known but are commonly attributed to reductions in the amount of bone remodeling in the body. Reductions in bone remodeling are believed to alter bone strength by causing reductions in the number and/or size of resorption cavities [3].

Reductions in bone turnover caused by anti-resorptive agents may occur through a reduction in the number of remodeling events, a reduction in the size of individual remodeling events (depth, breadth) or both. Alterations in the number and size of resorption cavities may change their effects as stress risers in cancellous bone or increase the likelihood that a remodeling event will fenestrate individual trabeculae [4]. Traditional, two-dimensional bone histomorphometry does not differentiate between a reduction in the number of individual remodeling events and a reduction in the size of individual remodeling events, but differences in number and size represent distinct differences in bone biomechanics [4, 5].

There are differences among anti-resorptive treatments that have the potential to alter bone biomechanical performance. Allen and colleagues found that dogs treated with raloxifene showed greater increases in vertebral bone strength per unit bone mineral density than untreated animals or animals treated with more potent anti-resorptive agents (alendronate) [6]. That raloxifene was associated with increased bone strength per unit BMD as compared to animals with greater rates of bone turnover (untreated controls) as well as animals with less bone turnover (alendronate treated) suggests that the biomechanical effects of anti-resorptive treatments may differ, independent of BMD and the degree to which they reduce bone turnover. Although changes in tissue material properties are a likely contributor to changes in biomechanical properties independent of BMD, alterations in the size of resorption cavities/remodeling events may also contribute to changes in cancellous bone biomechanics [7].

Studies using two-dimensional histomorphometry have reported that anti-resorptive treatment is associated with a reduction of resorption cavity size [8–15]. Although two-dimensional measures of average cavity depth (erosion depth, E.De) in a specimen are well established, the technique has been criticized and has been limited to a few practitioners [16]. Measures of the surface area of individual resorption cavities and formation events estimated from simple perimeter measures in two-dimensional sections violate stereological assumptions and are therefore biased [17] (see [18] for more discussion of the limitations of two-dimensional measures of resorption cavities). Recently, we applied a three-dimensional dynamic bone histomorphometry approach to the ovariectomized rat, and found that established estrogen deficiency in rats is associated with a reduction in the number of resorption cavities and formation events in vertebral cancellous bone, but not changes in the size of individual resorption cavities (including cavity width and depth) and few changes in formation event size [19]. To the authors' knowledge, no studies have used three-

dimensional imaging to assess the size of resorption cavities and formation events in animals treated with anti-resorptive agents.

Given our previous observation that the size of resorption cavities is not altered by a state of estrogen depletion (ovariectomy), we expect that a selective estrogen receptor modulator (raloxifene) will not have an effect on the size of resorption cavities. In contrast, we expect that a bisphosphonate (risedronate) will reduce the size of resorption cavities in three-dimensions because bisphosphonates have direct effects on osteoclasts. The long-term goal of the current line of investigation is to understand how changes in bone turnover influence bone biomechanics and fracture risk. In the current study we use an animal model of established estrogen depletion and a three-dimensional dynamic bone histomorphometry approach to determine the effect of anti-resorptive treatment on: 1) the size of individual resorption cavities (including depth, breadth and volume); and 2) the size of individual bone formation events.

2.0 MATERIAL AND METHODS

2.1 Image Acquisition and Processing

A total of 22, six month old female Sprague-Dawley rats were subjected to either bilateral ovariectomy (n=17) or sham surgery (SHAM, n=5). After allowing bone loss for one month, the ovariectomized animals were divided into three groups: no treatment (OVX, n=5), or three months of treatment with raloxifene (OVX+Ral, n=6) or risedronate (OVX+Ris, n=6, Figure 1). Raloxifene and risedronate were selected because they characterize two different classes of anti-resorptive treatment (SERM and bisphosphonate). Raloxifene was selected as it is the only SERM currently used clinically for the treatment of osteoporosis, while risedronate was selected because it is a less potent anti-resorptive agent than other bisphosphonates, allowing for a more direct comparison to raloxifene. Raloxifene (Sigma-Aldrich, St. Louis, MO, USA) was dissolved in deionized water at 1 g/mL and dosed at 1.5 mg/kg, 3× per wk. by oral gavage. Risedronate (Proctor & Gamble, Cincinnati, OH, USA) was dissolved in deionized water at 0.1 mg/mL and dosed at 5 µg/kg, 3× per wk. by subcutaneous injection (see Figure 1). Dosages of raloxifene and risedronate for rats were recommended by pharmaceutical companies (Eli Lilly and Co., Indianapolis, IN, USA, Proctor & Gamble) to simulate clinical doses for the treatment of postmenopausal osteoporosis. Animals were subjected to bone formation double labeling with xylenol orange (90 mg/kg) followed by calcein (10 mg/kg) at 10 and 3 days before euthanasia. Ovariectomy was confirmed using measures of uterine mass. Animals from the SHAM and OVX groups were described in a previous publication [19]. Animal use was performed under IACUC approval.

Following euthanasia, the lumbar vertebrae were dissected free of soft tissue. The cranial and caudal endplates of one lumbar vertebra from each animal (L3 or L4) were removed with a low-speed diamond saw and the marrow was washed out using a low pressure water jet. The undecalcified vertebrae were then embedded in opaque methyl-methacrylate and three-dimensional images of the vertebrae were collected using serial milling, as previously described [19, 20]. Serial milling involves repeatedly removing the top 5 µm from a plastic embedded specimen and collecting a mosaic of images of the newly revealed block face using epifluorescence microscopy. In the current study, serial milling was used to collect three fluorescent images (one for bone and one for each of the two bone formation labels) at a voxel size of $0.7 \times 0.7 \times 5.0$ µm [19]. Raw images collected using serial milling occupied 290–390 GB per specimen. Pre-processing steps were performed to tile the mosaic, crop the raw image to the size of the specimen and to remove noise caused by fluorescent signal originating beneath the optical plane [20]. Images were manually thresholded to obtain binary images of bone and each of the two bone formation markers (xylenol orange and

calcein). A region of interest more than 1 mm from the growth plate and $1\text{ mm} \times 1\text{ mm} \times 2\text{ mm}$ (height) in size was selected from the center of the vertebral body on the caudal side. The region of interest size has been shown to be sufficient for characterizing remodeling in a specimen using three-dimensional dynamic bone histomorphometry [19].

2.2 Three-dimensional measurements of bone remodeling

Three-dimensional measures of resorption cavities were achieved through manual tracing by a trained observer. Because manual tracing of resorption cavities in three-dimensional images is labor intensive, only a subset of all resorption cavities were examined using the following sampling strategy [18]: six independent uniform random transverse slices from each specimen were selected (each slice $300\text{ }\mu\text{m}$ from the next). An observer identified all eroded surfaces within a slice and the location of the eroded surface was recorded. A three-dimensional image of the neighborhood surrounding each identified eroded surface was displayed and the resorption cavity was traced in the three-dimensional image [21] (Figure 2). Our method achieved a sampling of 8–32 resorption cavities in each specimen. A three-dimensional spline was fit over the cavity to estimate the bone surface existing before resorption began to allow automated measures of cavity depth [19]. The mean and maximum depth of each cavity was determined. Cavity surface area (the area traced by the observer) and cavity volume were also determined. Three-dimensional dynamic bone histomorphometry was used to measure the number and surface area of individual formation events (double-labeled) and to measure mineral apposition rate in the three-dimensional images (See Figure 3 for three-dimensional images of cancellous bone specimens with bone formation labels) [19]. Following standard sampling rules formation event size was measured only in formation events entirely within the region of interest. A total of 7–82 double-labeled formation events entirely within the region of interest were measured in each specimen. Interobserver repeatability using these techniques has been previously characterized [19–21].

The eroded surface in the entire specimen (ES/BS) was measured using line intersection counting in two-dimensional sections (the six transverse cross-sections, grid with lines spaced $50\text{ }\mu\text{m}$ apart). Additionally, the percent double-labeled surface (dLS/BS) was calculated from the three-dimensional images. Three-dimensional measures of bone microarchitecture (BV/TV, Tb.Sp, etc.) were measured using BoneJ after coarsening images to $5.0 \times 5.0 \times 5.0\text{ }\mu\text{m}$ voxels [22].

Differences in bone microarchitecture, dLS/BS, MS/BS, BFR/BS and ES/BS among the four groups (SHAM, OVX, OVX+Ral, OVX+Ris) were identified with the non-parametric Kruskal-Wallis technique using Dunn's multiple comparisons test. Differences in formation event or resorption cavity size among groups were determined using a generalized least squares regression model to perform ANOVA including donor as a random effect to account for repeated measures within each animal (i.e. multiple formation events and cavities within each specimen). Multiple comparisons were performed using the Holm post-hoc test.

3.0 RESULTS

At four months after surgery, ovariectomized animals showed reduced bone volume fraction and bone-specific surface as compared to sham-operated controls ($p < 0.05$). Ovariectomized animals treated with raloxifene for three months showed reduced eroded surface (ES/BS) as compared to untreated ovariectomized animals ($p = 0.04$) but no significant differences in double-labeled surface (dLS/BS). Raloxifene treatment also led to a reduction in trabecular separation compared to untreated ovariectomized animals ($p = 0.02$) (Figure 4). Ovariectomized animals treated with risedronate for three months had reduced ES/BS as compared to untreated ovariectomized animals ($p = 0.02$) (Figure 4). Risedronate treatment

resulted in a reduction in double-labeled surface (dLS/BS, $p < 0.01$), mineralizing surface (MS/BS, $p = 0.02$) and bone formation rate (BFR/BS, $p = 0.05$) compared to untreated ovariectomized animals (Table 2). Trends suggested that anti-resorptive treatment increased bone volume fraction as compared to ovariectomized animals but were not considered statistically significant ($p > 0.05$).

Three-dimensional analysis of individual resorption cavities demonstrated no differences in cavity surface area (BS/Cv), maximum cavity depth (Cv.De), or cavity volume (Cv.V) between untreated ovariectomized animals and sham-operated controls. Ovariectomized animals treated with raloxifene or risedronate, however, showed 34.5–56.8% reductions in cavity surface area, maximum cavity depth and cavity volume as compared to untreated ovariectomized animals and sham controls ($p < 0.01$) (Table 1, Figure 5 A–B). Risedronate treatment was associated with reductions in mean depth per cavity as compared to both untreated ovariectomized animals and sham controls ($p < 0.01$). Raloxifene treatment was associated with reduced mean depth per cavity as compared to sham controls ($p < 0.01$). No differences in cavity morphology were observed between animals in the OVX+Ral and OVX+Ris groups (Table 1, Figure 5 A–B).

Surface area per double-labeled event (MS/dL.Ev) was greater in untreated ovariectomized animals compared to all other groups ($p < 0.01$). In addition, the risedronate treated group had reduced MS/dL.Ev compared to both sham controls and the raloxifene treated group ($p < 0.02$) (Table 2, Figure 5 D). Volume within each double-labeled formation event was reduced in animals treated with risedronate compared to other groups ($p < 0.01$) (Table 2). No differences in 3D mineral apposition rate were observed among the four groups (Figure 5 C). No significant differences the number of formation events per unit bone surface or in measurements of the size and number of single-labeled surfaces were observed between groups. As expected, median measures formation event size were correlated with dls/BS, and median measures of cavity size were correlated with ES/BS (See Figure S2 in supplementary materials).

4.0 DISCUSSION

Anti-resorptive agents can cause a fundamental change in the morphology of individual remodeling events, resulting in resorption cavities that are smaller in depth, volume and surface area as compared to ovariectomized animals and sham-operated controls. Furthermore, the anti-resorptive treatments examined here reduce the surface area of individual formation events as compared to untreated ovariectomized animals. The reduction in resorption cavity size with anti-resorptive treatment may not be correlated to the reduction in the total amount of bone remodeling, because cavity size is reduced during raloxifene treatment as compared to sham-operated controls while the total amount of bone turnover (characterized by ES/BS and dLS/BS) does not appear to differ between the two.

There are a number of strengths to the current study that provide confidence in our results. First, the current study is unique in using three-dimensional dynamic bone histomorphometry to examine differences in remodeling event size among treatments and therefore achieves the size and variability of individual events rather than specimen averages. Image processing and analysis using our three-dimensional approach has been validated thoroughly in a series of previous studies [19–21]. Second, the current study examined cavities that had been formed *in vivo*. Although three-dimensional studies of resorption cavity depth and breadth have been performed on cavities formed by osteoclasts *in vitro* [23–26] such measures are limited by culture conditions that do not exactly match the conditions *in vivo*. Lastly, the current study used older animals and began anti-resorptive

treatment after allowing bone loss to be established, thereby simulating the effects of treatment on a pre-existing state of osteopenia.

There are some limitations that must be considered when interpreting our results. First, we characterized the morphology of resorption cavities based on the observation of eroded surface and not on the presence of active osteoclasts, so our results are characteristic of cancellous bone morphology but are only indirect measures of bone resorption. It is possible to achieve three-dimensional images of resorption cavities identified with tartrate resistant acid phosphatase [27], but such approaches are labor intensive and to our knowledge have only been applied to a handful of cavities. Additionally, we measured only a subset of all resorption cavities in each specimen. Hence, we could not directly determine if the number of resorption cavities was altered with treatment. In a previous study in which we traced all resorption cavities in each specimen, we found that established estrogen deficiency resulted in an increase in the number of resorption cavities but no changes in cavity size (depth, surface area) [19]. Although ES/BS was reduced by both anti-resorptive agents ($p < 0.05$), the current study does not allow us to make conclusions regarding changes in the number of resorption cavities associated with anti-resorptive treatment. However, we were able to examine all bone formation events within the region of interest. While the number of bone formation events observed varied considerably (range 7–82), it did not differ between the four groups after accounting for differences in bone surface area.

Previous studies using two-dimensional histomorphometry approaches have suggested that anti-resorptive agents cause 10–30% reductions in average cavity depth and 20–30% reductions in cavity breadth (only two studies examined cavity breadth) [9–15]. In comparison, the current study found more pronounced reductions in resorption cavity size including a 35–51% reduction in depth and reductions in resorption cavity surface area of 47–57%. To the authors' knowledge, no studies have measured changes in the size of bone formation events following anti-resorptive treatment. The current study is the first to use three-dimensional approaches to analyze the effects of anti-resorptive agents on the surface area and volume of individual resorption cavities and formation events. In comparison to previous work the current study does not require stereology or selection of only cavities ideal for measurement (which introduces selection bias [16]).

The mechanism through which resorption cavities are reduced in size is not clear, but could be caused by changes in the number of osteoclasts at each resorption site, the amount of bone resorption by each osteoclast, the lifespan of osteoclasts at resorption sites or some combination of the three. Nitrogen containing bisphosphonates such as risedronate have been shown to reduce osteoclast function/lifespan, primarily by inhibiting GTPases that regulate osteoclast cytoskeletal rearrangement, membrane ruffling and vesicular trafficking necessary for bone resorption [28]. Recent work has shown that osteoclasts from mice deficient in Rac1 and Rac2 form smaller resorption cavities *in vitro* [26] which is consistent with the idea that risedronate treatment regulates cavity size by impairing osteoclast function. In contrast, our finding that raloxifene also leads to reductions in cavity size as compared to both SHAM and OVX animals is surprising because raloxifene is believed to act primarily as a replacement for estrogens and was therefore expected to reverse any changes in bone remodeling associated with ovariectomy. Since there was no difference in cavity size between the SHAM and OVX groups, we expected that raloxifene would not alter cavity size. There are two possible explanations for the changes in cavity size with raloxifene: First, it is possible that the reduction in size may be related to the timing of raloxifene dosage (3 times per week) leading to differences in the concentration of raloxifene in ovariectomized animals and circulating estrogens in SHAM operated animals. Second, others have noted subtle differences in the effects of raloxifene and estrogen on

bone remodeling [29, 30] and it is possible that alterations in the size of individual resorption cavities may be another difference between raloxifene and estrogen.

The current study is consistent with the idea that changes in resorption cavities may explain why reductions in fracture risk following anti-resorptive treatment are greater than expected from the associated changes in BMD. Reductions in maximum cavity depth and cavity volume associated with raloxifene and risedronate treatment are expected to reduce stress concentrations associated with resorption cavities, potentially providing benefits to bone strength independent of bone mineral density [4, 31]. Additionally, reductions in the maximum depth of resorption cavities may also reduce the likelihood that a resorption cavity disconnects or fenestrates a trabecula, helping to preserve cancellous bone microarchitecture over time. The magnitude of stress concentrations associated with resorption cavities depends on the number and size of resorption cavities, the location of the cavity within the structure (on a longitudinal trabecula vs. transverse trabecula, in a highly loaded or less loaded region of the microstructure) and local bone morphology (local trabecular thickness, plate-like vs. rod-like trabeculae, nodes in the structure, etc.) [4, 18]. Given the complex microarchitecture and load distribution within cancellous bone, additional biomechanical analyses are required to understand the mechanical consequences of resorption cavities.

In conclusion, our findings demonstrate that existing drug treatments have the ability to regulate the size of individual resorption cavities. Regulation of the size of individual resorption cavities may be one way in which anti-resorptive agents make cancellous bone more resistant to mechanical failure. Finally, regulating resorption cavity size has the potential to alter cancellous bone biomechanical performance in a way that may not be immediately apparent from measure of overall amounts of bone turnover.

Supplementary Material

Refer to Web version on PubMed Central for supplementary material.

Acknowledgments

This publication was made possible by AR057362 and AR054448 from NIAMS/NIH. Its contents are solely the responsibility of the authors and do not necessarily represent the official views of the NIAMS or NIH. The authors thank Proctor & Gamble for donating risedronate used in the study. The authors thank Amanda R. Bouman for assistance in image preparation.

Authors' roles: Study design: CJH, CRS, JBM, DWL. Data Collection: JBM, CRS, EVT, IL, KME, RET. Data Analysis: JBM, IL, CJH. Drafting of the manuscript: JBM, CJH. Revising manuscript content: JBM, DWL, CJH. Approving final version of the manuscript: JBM, CRS, EVT, IL, KME, RET, DWL, CJH. JBM and CJH take responsibility for the integrity of the data analysis.

REFERENCES

1. Cummings SR, Karpf DB, Harris F, Genant HK, Ensrud K, LaCroix AZ, Black DM. Improvement in spine bone density and reduction in risk of vertebral fractures during treatment with antiresorptive drugs. *Am J Med.* 2002; 112:281–289. [PubMed: 11893367]
2. Delmas PD, Li Z, Cooper C. Relationship between changes in bone mineral density and fracture risk reduction with antiresorptive drugs: some issues with meta-analyses. *J Bone Miner Res.* 2004; 19:330–337. [PubMed: 14969404]
3. Parfitt AM. High bone turnover is intrinsically harmful: two paths to a similar conclusion. The Parfitt view. *J Bone Miner Res.* 2002; 17:1558–1559. [PubMed: 12162510]
4. Hernandez CJ. How can bone turnover modify bone strength independent of bone mass? *Bone.* 2008; 42:1014–1020. [PubMed: 18373970]

5. Parfitt, AM. Skeletal heterogeneity and the purposes of bone remodeling. In: Marcus, R.; Feldman, D.; Nelson, DA.; Rosen, CJ., editors. Osteoporosis. 3rd Edition ed. San Diego, CA, USA: Elsevier Academic Press; 2008. p. 71-92.
6. Allen MR, Iwata K, Sato M, Burr DB. Raloxifene enhances vertebral mechanical properties independent of bone density. *Bone*. 2006; 39:1130–1135. [PubMed: 16814622]
7. Allen MR, Burr DB. Bisphosphonate effects on bone turnover, microdamage, and mechanical properties: what we think we know and what we know that we don't know. *Bone*. 2011; 49:56–65. [PubMed: 20955825]
8. Cohen-Solal ME, Shih MS, Lundy MW, Parfitt AM. A new method for measuring cancellous bone erosion depth: application to the cellular mechanisms of bone loss in postmenopausal osteoporosis. *J Bone Miner Res*. 1991; 6:1331–1338. [PubMed: 1792944]
9. Storm T, Steiniche T, Thamsborg G, Melsen F. Changes in bone histomorphometry after long-term treatment with intermittent, cyclic etidronate for postmenopausal osteoporosis. *J Bone Miner Res*. 1993; 8:199–208. [PubMed: 8442438]
10. Monier-Faugere MC, Friedler RM, Bauss F, Malluche HH. A new bisphosphonate, BM 21.0955, prevents bone loss associated with cessation of ovarian function in experimental dogs. *J Bone Miner Res*. 1993; 8:1345–1355. [PubMed: 8266826]
11. Wright CD, Garrahan NJ, Stanton M, Gazet JC, Mansell RE, Compston JE. Effect of long-term tamoxifen therapy on cancellous bone remodeling and structure in women with breast cancer. *J Bone Miner Res*. 1994; 9:153–159. [PubMed: 8140928]
12. Roux C, Ravaud P, Cohen-Solal M, de Vernejoul MC, Guillemant S, Cherruau B, Delmas P, Dougados M, Amor B. Biologic, histologic and densitometric effects of oral risedronate on bone in patients with multiple myeloma. *Bone*. 1994; 15:41–49. [PubMed: 8024850]
13. Boyce RW, Paddock CL, Gleason JR, Sletsema WK, Eriksen EF. The effects of risedronate on canine cancellous bone remodeling: three-dimensional kinetic reconstruction of the remodeling site. *J Bone Miner Res*. 1995; 10:211–221. [PubMed: 7754801]
14. Chavassieux PM, Arlot ME, Reda C, Wei L, Yates AJ, Meunier PJ. Histomorphometric assessment of the long-term effects of alendronate on bone quality and remodeling in patients with osteoporosis. *J Clin Invest*. 1997; 100:1475–1480. [PubMed: 9294113]
15. Allen MR, Erickson AM, Wang X, Burr DB, Martin RB, Hazelwood SJ. Morphological assessment of basic multicellular unit resorption parameters in dogs shows additional mechanisms of bisphosphonate effects on bone. *Calcif Tissue Int*. 2010; 86:67–71. [PubMed: 19953232]
16. Recker RR, Kimmel DB, Dempster D, Weinstein RS, Wronski TJ, Burr DB. Issues in modern bone histomorphometry. *Bone*. 2011; 49:955–964. [PubMed: 21810491]
17. Hauge EM, Mosekilde L, Melsen F. Stereological considerations concerning the measurement of individual osteoid seams and resorption cavities. *Bone Miner*. 1994; 26:89–90. [PubMed: 7832861]
18. Goff MG, Slyfield CR, Kummari SR, Tkachenko EV, Fischer SE, Yi YH, Jekir MG, Keaveny TM, Hernandez CJ. Three-dimensional characterization of resorption cavity size and location in human vertebral trabecular bone. *Bone*. 2012; 51:28–37. [PubMed: 22507299]
19. Slyfield CR, Tkachenko EV, Wilson DL, Hernandez CJ. Three-dimensional dynamic bone histomorphometry. *J Bone Miner Res*. 2012; 27:486–495. [PubMed: 22028195]
20. Slyfield CR Jr, Niemeyer KE, Tkachenko EV, Tomlinson RE, Steyer GG, Patthanacharoenphon CG, Kazakia GJ, Wilson DL, Hernandez CJ. Three-dimensional surface texture visualization of bone tissue through epifluorescence-based serial block face imaging. *J Microsc*. 2009; 236:52–59. [PubMed: 19772536]
21. Tkachenko EV, Slyfield CR, Tomlinson RE, Daggett JR, Wilson DL, Hernandez CJ. Voxel size and measures of individual resorption cavities in three-dimensional images of cancellous bone. *Bone*. 2009; 45:487–492. [PubMed: 19482097]
22. Doube M, Klosowski MM, Arganda-Carreras I, Cordelieres FP, Dougherty RP, Jackson JS, Schmid B, Hutchinson JR, Shefelbine SJ. BoneJ: Free and extensible bone image analysis in ImageJ. *Bone*. 2010; 47:1076–1079. [PubMed: 20817052]
23. Boyde A, Jones SJ. Pitfalls in pit measurement. *Calcif Tissue Int*. 1991; 49:65–70. [PubMed: 1913296]

24. Suzuki K, Takeyama S, Kikuchi T, Yamada S, Sodek J, Shinoda H. Osteoclast responses to lipopolysaccharide, parathyroid hormone and bisphosphonates in neonatal murine calvaria analyzed by laser scanning confocal microscopy. *J Histochem Cytochem*. 2005; 53:1525–1537. [PubMed: 16087705]
25. Soe K, Andersen TL, Hobolt-Pedersen AS, Bjerregaard B, Larsson LI, Delaisse JM. Involvement of human endogenous retroviral syncytin-1 in human osteoclast fusion. *Bone*. 2011; 48:837–846. [PubMed: 21111077]
26. Goldberg SR, Georgiou J, Glogauer M, Grynblas MD. A 3D scanning confocal imaging method measures pit volume and captures the role of Rac in osteoclast function. *Bone*. 2012; 51:145–152. [PubMed: 22561898]
27. Andersen TL, Sondergaard TE, Skorzynska KE, Dagnaes-Hansen F, Plesner TL, Hauge EM, Plesner T, Delaisse JM. A physical mechanism for coupling bone resorption and formation in adult human bone. *Am J Pathol*. 2009; 174:239–247. [PubMed: 19095960]
28. Russell RG, Xia Z, Dunford JE, Oppermann U, Kwaasi A, Hulley PA, Kavanagh KL, Triffitt JT, Lundy MW, Phipps RJ, Barnett BL, Coxon FP, Rogers MJ, Watts NB, Ebetino FH. Bisphosphonates: an update on mechanisms of action and how these relate to clinical efficacy. *Ann N Y Acad Sci*. 2007; 1117:209–257. [PubMed: 18056045]
29. Taranta A, Brama M, Teti A, De luca V, Scandurra R, Spera G, Agnusdei D, Termine JD, Migliaccio S. The selective estrogen receptor modulator raloxifene regulates osteoclast and osteoblast activity in vitro. *Bone*. 2002; 30:368–376. [PubMed: 11856644]
30. Rogers A, Clowes JA, Pereda CA, Eastell R. Different effects of raloxifene and estrogen on interleukin-1beta and interleukin-1 receptor antagonist production using in vitro and ex vivo studies. *Bone*. 2007; 40:105–110. [PubMed: 16934544]
31. Dempster DW. The contribution of trabecular architecture to cancellous bone quality. *J Bone Miner Res*. 2000; 15:20–23. [PubMed: 10646110]

Highlights

- We examine the size of resorption cavities in 3D following antiresorptive treatment
- We examine the size of formation events in 3D following antiresorptive treatment
- Raloxifene and risedronate treatment reduced resorption cavity size in OVX rats
- Antiresorptive treatment may reduce cavity size independent of bone turnover
- Reduced cavity size may contribute to reduced fracture risk following treatment

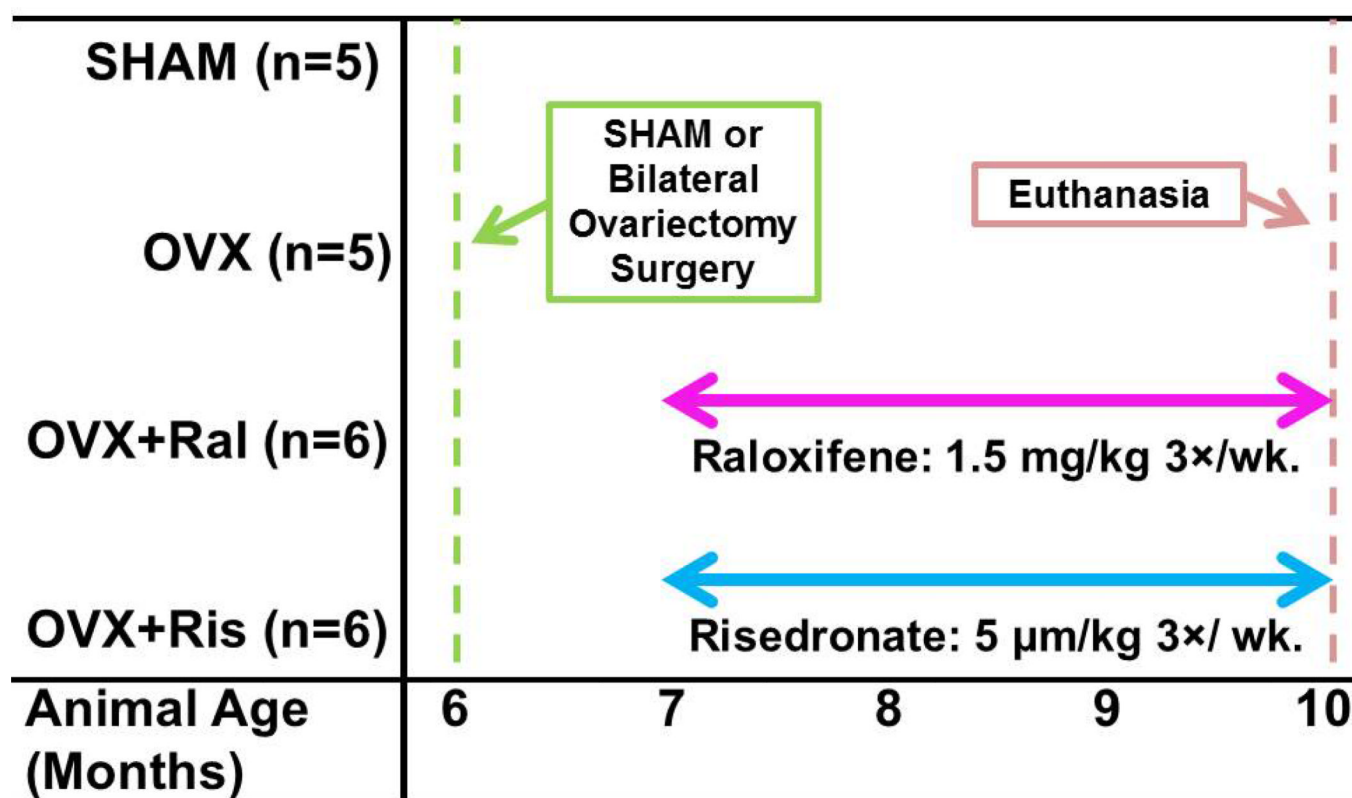


Figure 1.
The timing of surgery and treatment in the study design are illustrated.

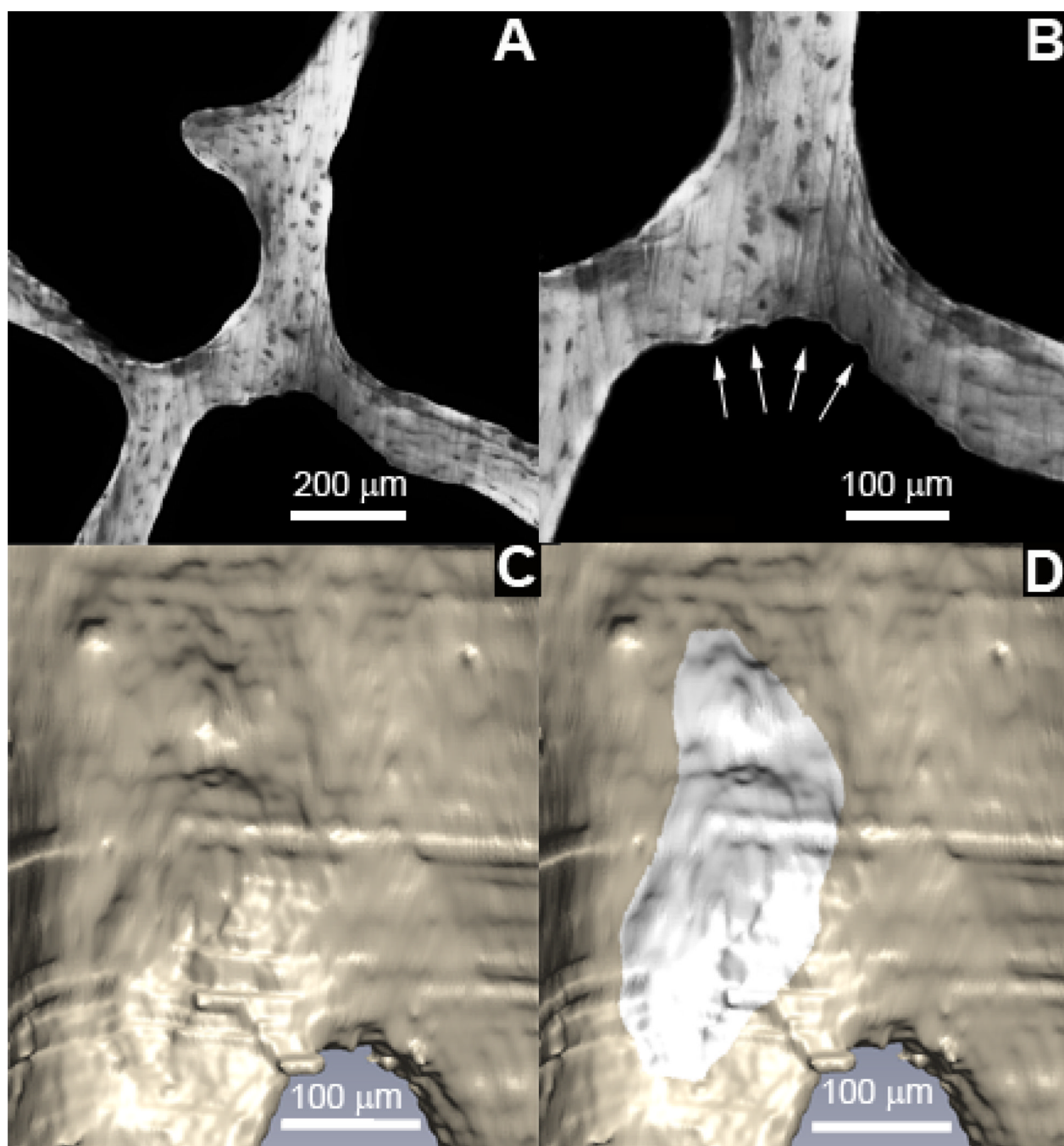


Figure 2. Resorption cavities were identified as eroded surfaces in gray scale images (A) after examination at 2× magnification (B). Cavities were visualized in three-dimensions (C) and traced by a trained observer using gray scales images and the three-dimensional surface (D).

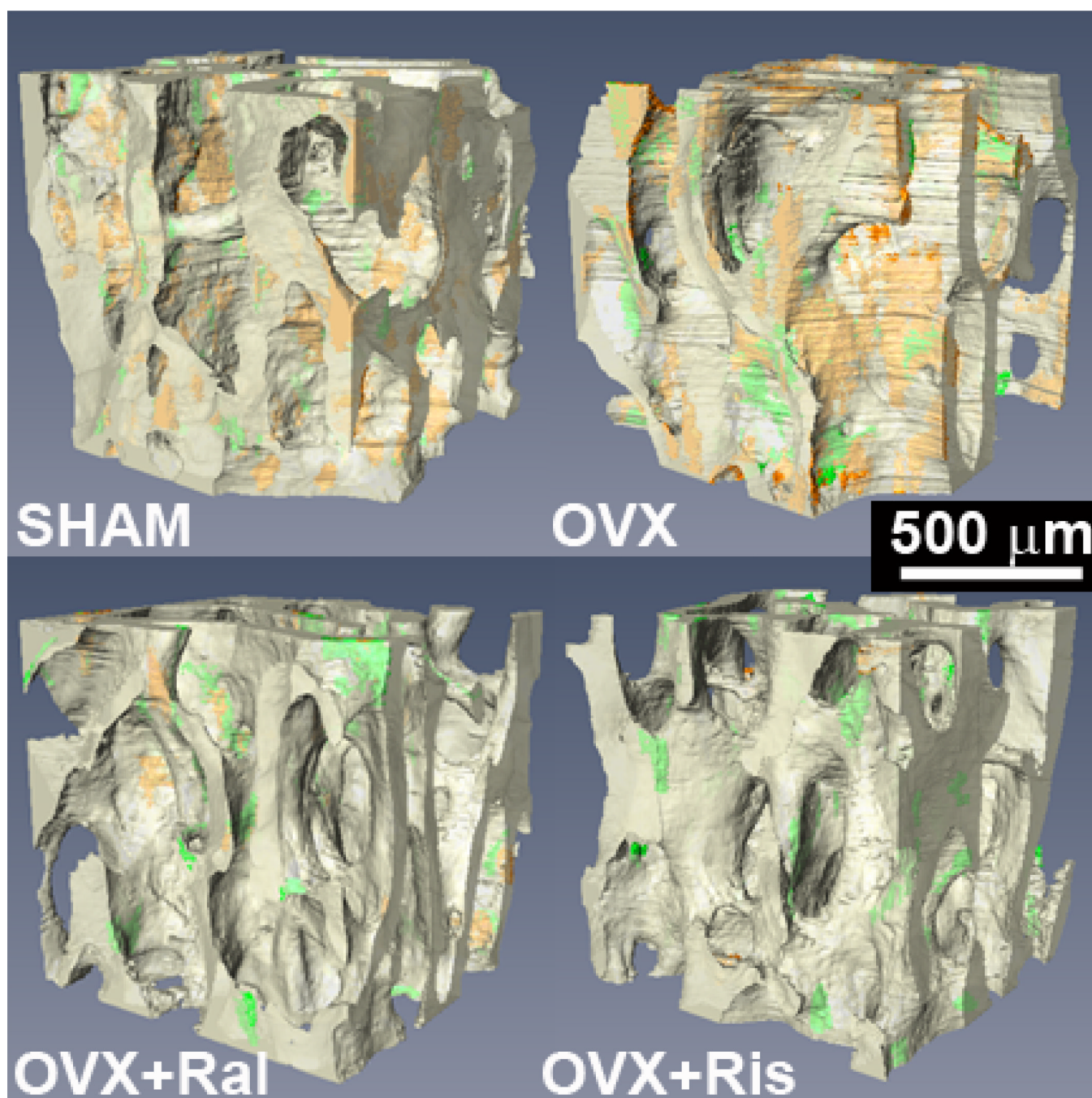


Figure 3. Three-dimensional images of cancellous bone from the rat lumbar vertebrae for the four groups are shown with transparency to show regions of the first bone formation label (xylene orange) and the second formation label (calcein green).

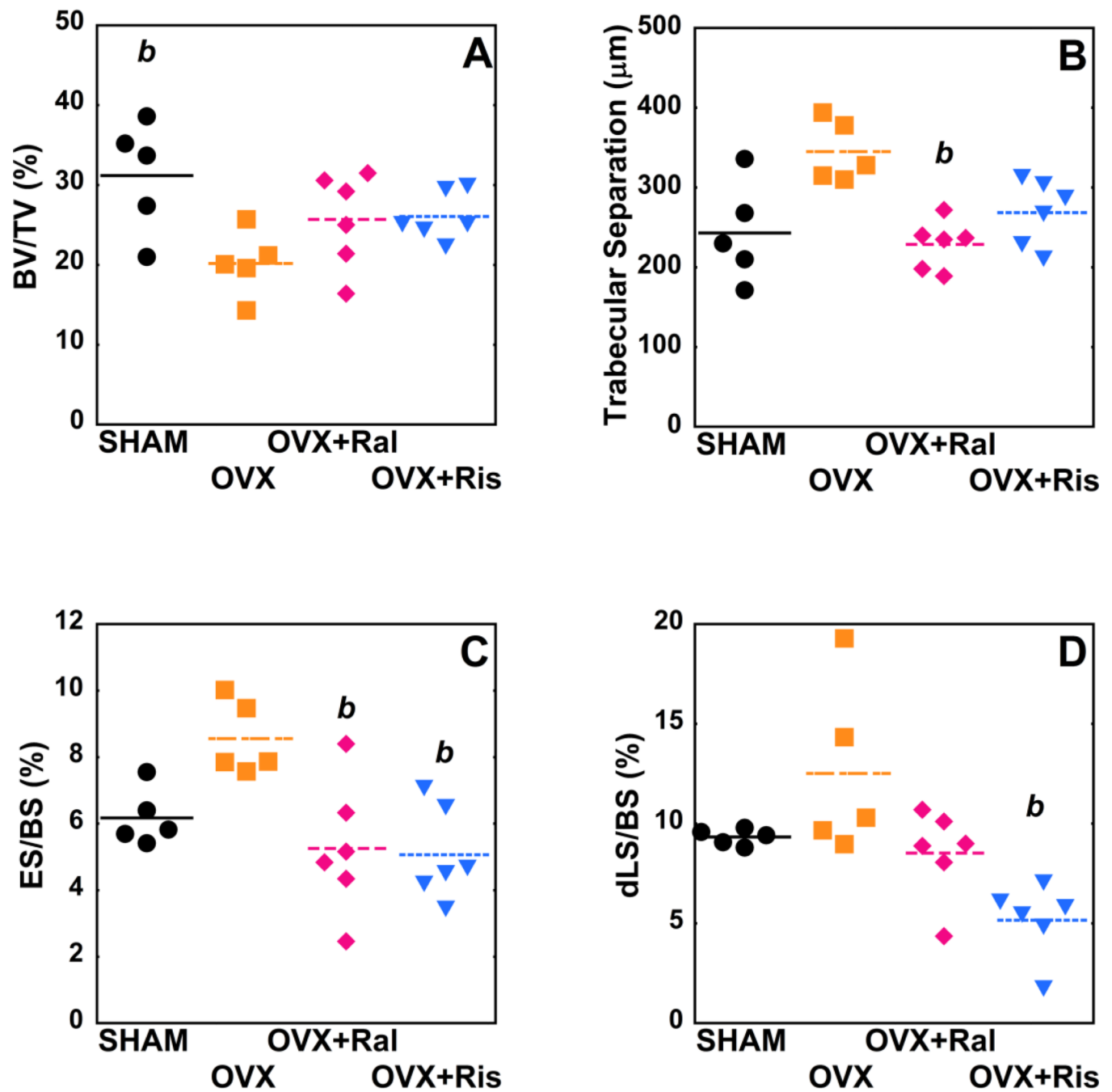


Figure 4.

Whole specimen measures of bone microarchitecture and remodeling are shown for each of the study groups ($p < 0.05$), (A) BV/TV, (B) Tb.Sp, (C), ES/BS (D) dLS/BS. Differences between groups analyzed using, Dunn's multiple comparison test. b- $p < 0.05$ vs. OVX untreated.

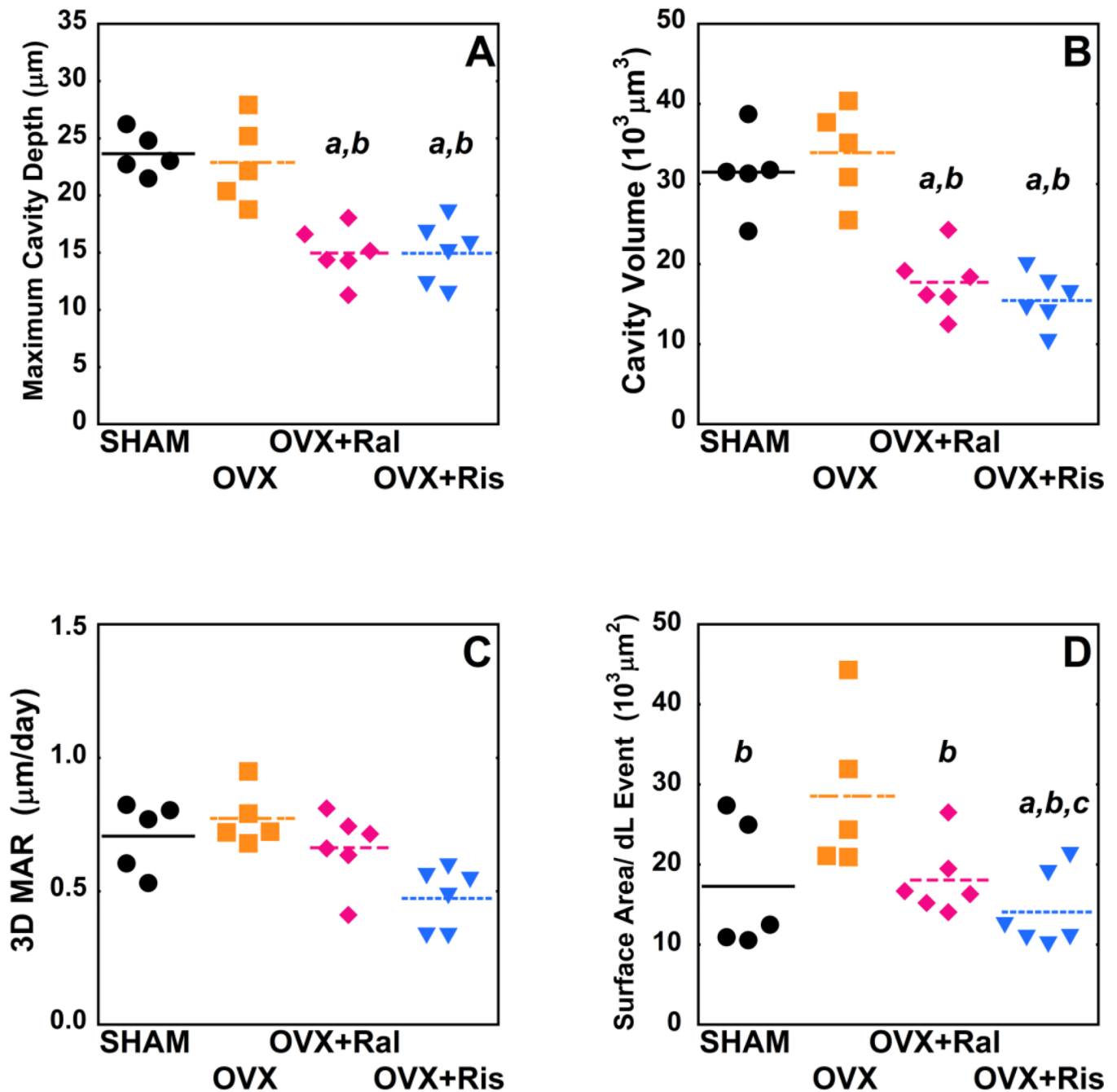


Figure 5.

Median measurements of individual resorption cavities and formation events are shown for each of the study groups ($p < 0.05$), (A) Cv.De, (B) Cv.V, (C), 3D MAR (D) MS/dL.Ev.

Statistical differences are shown based on generalized least squares regression models that include all events and donor as a random effect. a- $p < 0.05$ vs. SHAM operated, b- $p < 0.05$ vs. OVX untreated, and c- $p < 0.05$ vs. OVX+Ral.

Table 1

Static Histomorphometry measures for each group are shown, Mean \pm SD across animals within a group, 95% CI (5th, 95th).

Measurement	SHAM (n=5)	OVX (n=5)	OVX+Ral (n=6)	OVX+Ris (n=6)
Bone volume fraction (BV/TV, %)	31.18 \pm 6.99 (22.50, 39.86) ^b	20.18 \pm 4.08 (15.12, 25.24)	25.68 \pm 5.92 (19.47, 31.90)	26.05 \pm 3.01 (22.89, 29.21)
Bone-specific surface (BS/BV, mm ⁻¹)	9.58 \pm 1.65 (7.53, 11.63) ^b	6.98 \pm 1.11 (5.60, 8.36)	9.03 \pm 1.18 (7.80, 10.27)	8.38 \pm 0.76 (7.59, 9.18)
Trabecular thickness (Tb.Th, μ m)	87.52 \pm 7.57 (78.13, 96.92)	76.14 \pm 3.20 (72.17, 80.12)	75.13 \pm 14.58 (59.83, 90.43)	83.59 \pm 8.83 (74.33, 92.85)
Trabecular separation (Tb.Sp, μ m)	243.01 \pm 62.92 (164.89, 321.14)	344.83 \pm 38.32 (297.25, 392.42)	228.51 \pm 30.29 (196.72, 260.29) ^b	268.74 \pm 41.10 (225.61, 311.87)
Structural modeling index (SMI)	1.16 \pm 0.27 (0.82, 1.50)	1.47 \pm 0.37 (1.02, 1.93)	1.48 \pm 0.34 (1.12, 1.83)	1.44 \pm 0.11 (1.33, 1.56)
Degree of anisotropy (DA)	0.68 \pm 0.12 (0.53, 0.83)	0.65 \pm 0.08 (0.55, 0.75)	0.72 \pm 0.06 (0.65, 0.79)	0.67 \pm 0.12 (0.54, 0.80)
*Eroded surface (ES/BS, %)	6.17 \pm 0.85 (5.12, 7.23)	8.55 \pm 1.11 (7.17, 9.93)	5.26 \pm 2.00 (3.16, 7.35) ^b	5.06 \pm 1.41 (3.58, 6.54) ^b
[†] Median Maximum Cavity Depth (Cv.De, μ m)	23.66 \pm 1.87 (21.34, 25.97)	22.88 \pm 3.69 (18.30, 27.47)	14.96 \pm 2.30 (12.55, 17.38) ^{ab}	14.94 \pm 2.70 (12.11, 17.77) ^{ab}
[†] Median Mean Cavity Depth (μ m)	3.76 \pm 0.42 (3.23, 4.28)	3.20 \pm 0.88 (2.11, 4.29)	2.38 \pm 0.47 (1.89, 2.87) ^a	1.82 \pm 0.44 (1.36, 2.28) ^{ab}
[†] Median Cavity Surface Area (BS/Cv, 10 ³ μ m ²)	17.99 \pm 2.33 (15.11, 20.88)	19.76 \pm 3.02 (16.01, 23.51)	9.59 \pm 2.24 (7.24, 11.94) ^{ab}	8.55 \pm 2.17 (6.28, 10.82) ^{ab}
[†] Median Cavity Volume (Cv.V, 10 ³ μ m ³)	31.49 \pm 5.18 (25.06, 37.92)	33.92 \pm 5.87 (26.63, 41.21)	17.73 \pm 3.96 (13.58, 21.89) ^{ab}	15.44 \pm 3.32 (11.95, 18.92) ^{ab}

* Measured in two-dimensions using line intersection

[†] Median of 8–32 cavities within a specimen

^a p<0.05 vs SHAM group

^b p<0.05 vs OVX group

Table 2

Dynamic bone histomorphometry measures are shown for each group, Mean \pm SD, 95% CI (5th, 95th).

Measurement	SHAM (n=5)	OVX (n=5)	OVX+Ral (n=6)	OVX+Ris (n=6)
Double-labeled surface (dLS/BS, %)	9.33 \pm 0.40 (8.84, 9.82)	12.51 \pm 4.32 (7.14, 17.88)	8.52 \pm 2.24 (6.17, 10.88)	5.16 \pm 1.83 (3.24, 7.09) ^b
Mineralizing surface (MS/BS, %)	11.45 \pm 0.76 (10.50, 12.39)	13.89 \pm 4.61 (8.17, 19.62)	10.38 \pm 2.71 (7.54, 13.22)	8.14 \pm 1.98 (6.06, 10.22) ^b
Single-labeled surface (sLS/BS, %)	4.23 \pm 2.19 (1.51, 6.95)	2.75 \pm 1.11 (1.38, 4.13)	3.71 \pm 2.26 (1.34, 6.08)	6.06 \pm 1.94 (4.02, 8.10)
No. of double-labeled formation events (N.dL.Ev)	59.20 \pm 33.54 (17.55, 100.85)	29.40 \pm 8.68 (18.63, 40.17)	38.50 \pm 16.16 (21.54, 55.46)	25.17 \pm 13.56 (10.94, 39.39)
No. of single-labeled formation events (N.sL.Ev)	114.00 \pm 63.52 (35.13, 192.87)	49.60 \pm 18.74 (26.33, 72.87)	77.50 \pm 29.15 (46.91, 108.09)	110.33 \pm 32.32 (76.42, 144.25)
No. of double-labeled formation events per unit bone surface (N.dL.Ev/BS, mm ⁻²)	3.20 \pm 1.32 (1.55, 4.84)	2.23 \pm 0.54 (1.56, 2.90)	2.25 \pm 0.87 (1.34, 3.17)	1.63 \pm 0.98 (0.61, 2.66)
No. of single-labeled formation events per unit bone surface (N.sL.Ev/BS, mm ⁻²)	6.50 \pm 3.61 (2.02, 11.00)	3.76 \pm 1.27 (2.19, 5.34)	4.63 \pm 1.89 (2.64, 6.61)	6.96 \pm 1.66 (5.21, 8.71)
$\dot{\gamma}$ Median 3D mineral apposition rate (3D MAR, μ m/day)	0.71 \pm 0.13 (0.54, 0.87)	0.77 \pm 0.11 (0.64, 0.90)	0.66 \pm 0.14 (0.52, 0.81)	0.47 \pm 0.11 (0.35, 0.59)
Bone formation rate (BFR/BS, μ m/day)	0.11 \pm 0.03 (0.07, 0.15)	0.13 \pm 0.05 (0.07, 0.19)	0.09 \pm 0.04 (0.06, 0.13)	0.05 \pm 0.02 (0.04, 0.07) ^b
$\dot{\gamma}$ Median surface area per double-labeled event (MS/dL.Ev, 10 ³ μ m ²)	17.26 \pm 8.22 (7.06, 27.46) ^b	28.53 \pm 9.89 (16.25, 40.80)	18.05 \pm 4.53 (13.29, 22.80) ^b	14.05 \pm 4.77 (9.04, 19.05) ^{abc}
Median surface area per single-labeled event (MS/sL.Ev, 10 ³ μ m ²)	3.31 \pm 0.24 (3.01, 3.61)	3.98 \pm 0.41 (3.47, 4.49)	3.74 \pm 0.64 (3.08, 4.41)	4.34 \pm 0.56 (3.76, 4.93)

Measurement	SHAM (n=5)	OVX (n=5)	OVX+Ral (n=6)	OVX+Ris (n=6)
^{††} Median volume per double-labeled event (V/dL.Ev, 10 ³ µm ³)	80.76±41.33 (29.43, 132.08)	155.71±93.06 (40.16, 271.26)	91.75±29.20 (61.11, 122.39)	43.90±21.72 (21.11, 66.69) ^{abc}

^{††} Median of 7–82 formation events in each specimen

^a p<0.05 vs SHAM group

^b p<0.05 vs OVX group

^c p<0.05 vs OVX+Ral group